International Journal of Food Science +Technology

Institute of Food Science +Technology ifst



Original article

# Impact of the tiger-nut milk co-product on fibre-enriched bread processing and storage: crumb structure-moisture-texture relationships

**Samuel Verdú,[1]* Cecibel Alava,[1] José M. Barat,[1] Conrado Carrascosa[2]* & Raúl Grau[1]**

1 Departamento de Tecnología de Alimentos, Universitat Politècnica de València, Valencia, Spain
2 Departamento de Patología Animal, Producción Animal, Bromatología y Tecnología de los Alimentos, Universidad de Las Palmas de Gran Canaria, 35413 Arucas, Las Palmas, Spain

*(Received 5 October 2022; Accepted in revised form 4 December 2022)*

**Summary** The effect of including tiger-nut milk co-product on the bread-making process was studied. The impact of three wheat flour substitution co-product levels (5%, 10% and 20%) was tested by comparing to a control (pure wheat) as regards fermentation kinetics and baking phase, as well as their implications on the physicochemical features of breads (crumb internal structure, moisture and texture distribution) just after processing and during storage. The dough fermentation kinetics showed significant differences: reducing maximum height at 60 min and maximum growth rate with an increasing co-product concentration. However, water retention in baking was the same for them all despite their differences in volume. These facts significantly affected the crumb internal structure, which was successfully characterised by an image analysis technique. Crumb moisture-structure-texture relationships were analysed in two different zones of cross-section bread slices. The results showed how an increasing co-product level enhanced the homogenization of moisture distribution and hardness across crumb zones, and also reduced the structure differences between them. Moisture and hardness presented high correlation levels with changes in the structure of crumb zones during storage, which allowed the significant effect of co-product on the crumb moisture-structure-texture relationships to be knownin both the bread-making process and storage time.

**Keywords** Bread, fermentation kinetics, image analysis, internal structure, storage, tiger-nut milk co-product.

## Introduction

Incrementing dietary fibre intake is recommended by Health Authorities because population diet habits have shifted to products with high-fat and refined carbohydrate contents (Dhingra *et al*., 2012) which, in turn, rises calorie input and leads to poor nutritional contribution (López-Azpiazu *et al*., 2003). These diet habits have been reported to contribute to the risk of suffering several health diseases, like type II diabetes mellitus, hypertension, obesity and colon cancer (Muñoz *et al*., 2022).

Enriching the fibre content of food products with low-fibre content natively is an extended practice in industry (refined flours bakery, drinks, beverages, meat and dairy products) because it improves nutritional input, provides high-value products and contributes to competitiveness. These products have to follow the labelling regulations specified in Regulation (EC) No. 1924/2006 of the European Parliament on nutrition and health claims made on foods. It indicates that to label "source of fibre foods", a given product requires 3 g of fibre/100 g of product, while 6 g of fibre/100 g of product are required for "high-fibre content foods". However, significant changes across the process chain and sensorial properties could be induced with the incorporation of fibre into pre-established matrix products. With bread, the most affected features are those related with physico-chemical properties, such us moisture status, structural properties, rheological behaviour, heat conductivity, water retention, texture parameters, colour, *etc*. (Barros *et al*., 2018; Alba *et al*., 2020). Therefore, studying the impact of incorporating fibre sources into specific products with considerable difficulties because of morphological and sensorial properties or process operations is an important experimentation area.

*Correspondent: E-mail: saveram@upvnet.upv.es, conrado.carrascosa@ulpgc.es

doi:10.1111/ijfs.16248

In the food industry there is a marked tendency to recover from secondary products the valuable compounds contained in food processing waste which, in many cases, represent a rich dietary fibre source. These co-products can be transformed into profitable compounds as raw materials for secondary processes (intermediate compounds), or as ingredients of new ingredients and foods (Sánchez-Zapata *et al*., 2009). Along these lines, the tiger-nut (*Cyperus esculentus*) co-product milk is an important source of fibre, which is traditionally used to organic material for composting, combustion and feed production purposes. This false nut is the tuber of a Corsa sedge genus perennial herb member of the grass family *Cyperaceae* (Barros *et al*., 2020). Interest in developing applications for this co-product also lies in the fact that several geographic zones of Spain, one of the world's main tiger-nut milk producers, generate large volumes of it. Tiger-nut milk production generates around 60% of harvested plant material (5.3 million of kg of dry tiger-nuts in 2016), the management of which is another problem for producers. Data about the impact of this co-product on some food properties, such as pork sausages, burgers and wheat based matrices, have been reported in several studies (Bobreneva & Baioumy, 2018; Alava *et al*., 2019), but very little information about its effect on the bread-making process is available. Some studies about the incorporation of tiger-nut into bread and cake-making exist, but only with the whole tuber flour (Aguilar *et al*., 2014). In that sense, increasing information about the effect of this type of co-product when included in fermented-based cereal products such as bread could help food producers to use it as a high-quality fibre source. That information should collect the response of this new ingredient at the main stages of the bread-making process. Thus, this work aimed to study the impact of including the tiger-nut milk co-product in the main bread-making process phases (fermentation and baking), its implications on internal bread structures, and its relationship with moisture distribution and textural properties during storage.

## Material and methods

### Flours

Breads were produced by mixing wheat flour with the tiger-nut milk co-product flour at three substitution levels, 5%, 10% and 20% w/w, on a dry basis (d.b) of the wheat flour. These substitution levels were selected following Regulation (EC) No. 1924/2006 of the European Parliament and European Council. It indicates parameters for both "source of fibre foods" that require 3 g of fibre/100 g of product and "high fibre content foods" that require 6 g of fibre/100 g of product. Thus the 5% substituted formula was in accordance with the first denomination, the 10% substituted formula was in accordance with the second one, and the 20% substituted formula was included to evaluate the behaviour and feasibility of a larger amount of fibre in the process. The employed commercial refined wheat flour was obtained from a local producer (Molí del Picó-Harinas Segura S.L. Valencia, Spain), whose chemical composition was: 1.2 ± 0.03% of fat, 14.7 ± 0.5% of proteins, 14.5 ± 0.4% of water, and 0.31 ± 0.1 of ash (w.b). The alveographic parameters were also facilitated by the company, and were: $L$ = 128 ± 5 (extensibility (mm)), $P$ = 94 ± 2 (maximum pressure (mm)), $W$ = 392 ± 11 (strength ($J^{-4}$)) and 0.73 of $P/L$.

The tiger-nut milk co-product was obtained from a local tiger-nut milk manufacturing plant, presented as wet fibrous flour. Two kinds of milled fibrous tissues can be differentiated in this co-product from a microscopic viewpoint (Fig. 1a). The first has a larger particle size and is brown(>800 μm), like any grain bran, and is provided by the periderm and the cortex of the tuber. It is a typical woody fraction characterised by a high lignin content, among other insoluble polymers. The second kind has a smaller particle size (<800 μm), is white, and is provided by internal tuber tissues, such as the perimedulla and medulla. It is a cotton-like material whose composition is based on insoluble carbohydrates, such as cellulose, hemicellulose and non-digestible starches (Sun *et al*., 2019). The co-product flour was dried to 14% of moisture (w.b) to be milled in a stainless steel grinder (Retsch GmbH, ZM 200, Haan, Germany) until around 271.1 ± 8.1 μm, expressed as the average total volume size of the analysed flour particles ($D$ *[4, 3]*). Finally, the proximate composition was 1.9 ± 0.7% of proteins, 13.3 ± 0.1% of fat, 14.1 ± 0.4% of water, 1.86 ± 0.1 of ash and 68.2 ± 0.4% of the total dietary fibre (w.b). This proximate composition was analysed based on ICC (International Association for Cereal Science and Technology) standards 110/1, 156, 136, 105/2 and 104/1 for water, dietary fibre, fat, protein and ash, respectively.

### The bread-dough processing phase

The formulation used to prepare the model dough was based on Verdú *et al*. (2017). It was as follows: 56% flour, 4% white sugar (≥ 99.8% of saccharose), 2% refined sunflower oil (maximum acidity 0.2° Koipesol Semillas, S.L., Spain), 2% commercial pressed yeast (*Saccharomyces cerevisiae*, Lesafre Ibérica, S.A., Spain), 1.5% salt (refined marine salt ≥97% NaCl) and added water 34.5% (w/w). It was not necessary to modify the added water percentage because both flours presented the same moisture at the time dough was produced.

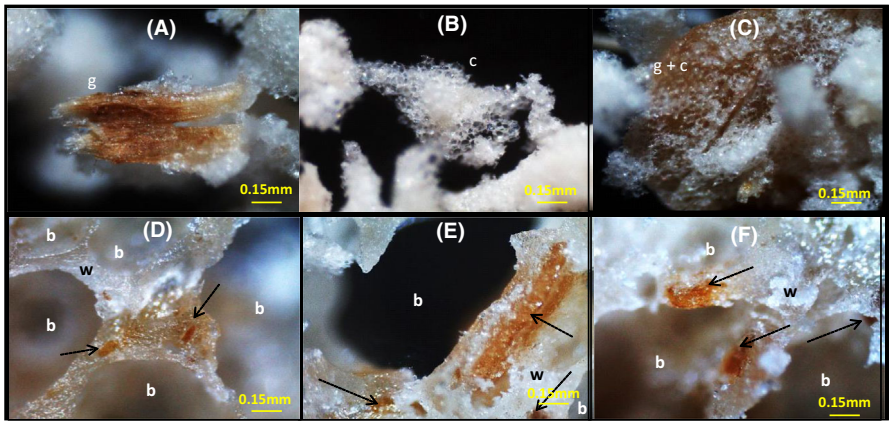


**Figure 1** Augmented views of the tissues contained in the tiger-nut milk co-product and breadcrumbs that contained the co-product. Fragment of the external and internal tiger-nut tissue, (A) lignin (external), (B) cellulose (internal), (C) both tissue types; (B) internal wall of breadcrumbs. (D–F): internal structure of crumb; b: bubble; w: matrix/bubble walls; black arrows indicate presence of co-product particles.

Bread dough was made according to a closed process, with no modifications between formulas. This process was done by mixing all the components in a food mixer (Thermomix® TM31, Vorwerk, Germany) according to this method: in the first phase, sugar, NaCl and liquid components (water and oil), were mixed for 4 min at 37 °C. Yeast was added in the next step to be mixed at the same temperature for 30 s. In the last step, flour was mixed according to a default dough mixing programme, which provides homogeneous dough. The programme system centres on mixing ingredients with random turns of the mixer helix in both directions (550 revolutions/min) to obtain homogeneous dough. This process was carried out for 4.5 min at 37 °C. Then 450 g of dough were prepared in the metal mould (8 × 8 × 30 cm) for fermentation phase. Dough height was approximately 1 ± 0.1 cm. Ten replicates of each bread formula were produced and analysed.

*Fermentation phase*

The fermentation phase was carried out in a chamber with controlled humidity and temperature (KBF720 Binder Tuttlingen, Germany); 37 °C and 90% relative humidity (RH) were the conditions used for 60 min. The growth kinetics of doughs were monitored by a laser distance measurer device (BOSCHGLM 50, 1.5 mm of accuracy, laser diode 635 nm) fitted and calibrated inside the chamber. Height was taken in the middle of the dough by taking the metal mould dimensions (width and length of the base) as a reference. Dough behaviour during fermentation was modelled using the adapted Gompertz prediction model. The Gompertz function is a non-linear sigmoid growth function developed by to calculate the mortality rate of microorganisms, however it has been applied to modelling multitude of phenomena with sigmoid behaviour (Chu, 2020). The equation is as follows:

$$H = \alpha \bullet \exp\left(-\exp\left(\frac{V}{\alpha}\bullet(Lt-t)+1\right)\right) \qquad (1)$$

where $H$ is calculated height, $t$ is a given time, $\alpha$ is the real height during the process at a given time, $V$ is the maximum growth rate, and $Lt$ represents the latency time before dough development begins. Model parameters were determined by a non-linear regression procedure and were obtained by minimising the sum of the squares from the prediction errors. Data from ten replicates of bread from each formula were collected.

*Baking phase*

The baking process was done at the end of fermentation phase. Moulds were positioned in the central zone of the oven plate (530 × 450 × 340, Rotisserie, DeLonghi, Italy), which was heated to 180 °C. Baking time was 35 min. Having finished this operation, breads were cooled for 30 min under room conditions (25 °C/70% R.H). The mass loss for each sample was calculated based on eq. 2:

$$\Delta M = \frac{m_t - m_0}{m_0} \bullet 100 \qquad (2)$$

where $\Delta M$ is the mass variation in % at a given time, $m_t$ is the mass of the sample at the end of cooling time and $m_o$ is the initial mass of the sample before baking. Data from ten replicates of bread from each formula were collected.

## Storage

Cooled breads were packed in a low-density polyethylene bag, similar to that used in commercial

presentations, and were stored under environmental conditions (23 °C and 72% RH, approximately) (Verdú *et al.*, 2015). Analytical determinations, e.g., moisture, textural analysis and image captions of crumbs, were carried out for 0, 3 and 6 days of storage. Ten replicates of each breads per formula were produced and five slices of each central bread zone were analysed.

### Analytical determinations of breads

*Specific volume*

Specific bread volumes were measured by the millet seed displacement method (AACC Method 10–05.01). Then the specific volume ($Sv$) was calculated as the ratio between volume (mL) and bread weight (g). Increments in the specific volume compared to the control ($\Delta Sv$) were also calculated as %. Specific volumes of ten replicates of bread from each formula were analysed.

*Texture profile analysis*

Textural properties were analysed in two breadcrumb zones, A and B, which respectively correspond to the upper and bottom bread slice zones. Texture profile analyses ($TPA$) were run by taking 1.5 × 1.5 cubes from bread zones A and B (see Appendix S1). Assays were carried out in a TA-TX2 texture analyser (Stable Micro Systems, Surrey, UK). A 25-kilogram load cell and a 35-mm diameter probe were used. The assay speed was set at 1.7 mm/s to compress crumb cubes at 50% of their previous height. The time between compressions was 5 s. The studied parameter was mainly hardness ($D$), but the other TPA parameters are included in the Appendix S1 (gumminess ($G$), chewiness ($Ch$) and resilience ($R$)). Five samples of the ten bread samples from each formula were analysed.

*Moisture*

The moisture content ($X_w$) of the entire breads and crumb cubes from zones A and B were determined according to ICC (International Association for Cereal Science and Technology) Standard 136.

*Crumb image analysis*

In order to study the changes produced in bread crumb structures from introducing the co-product, a 2D image from the 1.5 cm-thick slices of central bread zones was obtained. The capture system was a HD webcam C615 (Logitech) fixed to a rigid structure that left 20 cm of samples, and a LED lamp IP20 5 W was used as the lighting system. On the camera capture scene, a black matte material was placed to reduce any reflections on the camera. The camera took fine quality pictures of 3264 × 2448 pixels in the JPEG format. Images were processed by adapting the method described by Zheng *et al.* (2011). This process applies the fractal analysis to evaluate the complex structure patterns presented in each image and to obtain information about their plausible modifications. The basic procedure was:

1 Images were converted into an 8 bits *greyscale* (Fig. 2a)
2 Each image was thresholded and segmented for each grey value between 0 (black extreme) and 255 (white extreme) (Fig. 2b).
3 Fractal information was based on the fractal dimension ($Fd$) parameter, which was obtained by the box-counting method (Panigrahy *et al.*, 2020). It was calculated for each grey value of every image. Images were divided into square sub-boxes with a variable length denoted as box size ($\varepsilon$). The $\varepsilon$ number this study was 10, which expressed the % of the image width as: 0.5, 5, 10, 15, 20, 25, 30, 35, 40 and 50. Thus the number of boxes that contain pixels is counted for each $\varepsilon$, and called $N\varepsilon$. The relationship between $\varepsilon$ and $N\varepsilon$ could be described by the following equation:

$$log N\epsilon = -Fd \bullet log\epsilon + a \quad (3)$$

where $a$ is the constant, and $Fd$ is the fractal dimension of the divided image. Then $Fd$ is the slope of the obtained regression line (De Melo & Conci, 2013). Finally, an $Fd$ spectrum of each image were obtained (Fig. 2c). Ten breads per formula were studied by five slices of each central bread zone.

Images were used to extract information about both entire slice structures, and about two different zones. Those zones were the upper zone (A) and the bottom zone (B), and each was selected as the area collected within 50% of slice height. These image analyses were performed using FracLac for ImageJ created by Karperien (2013).

### Statistical analysis

The fermentation and bread properties data were studied by a one-way variance study (ANOVA). In those cases with a significant effect ($P$-value <0.05), the average was compared by Fisher's least significant difference (LSD). The study of bread crumb structures was conducted with the fractal analysis data from the crumb images using a Principal Component Analysis ($PCA$) and Support Vector Machines ($SVM$) for regression ($SVM$-$R$). $PCA$ is a multivariate unsupervised statistical method used to describe and reduce the dimensionality of a large set of quantitative variables to a small number of new variables, called principal components (PCs), which are the result of linear combinations of the original variables. $SVM$ is a supervised learning methodology based on the

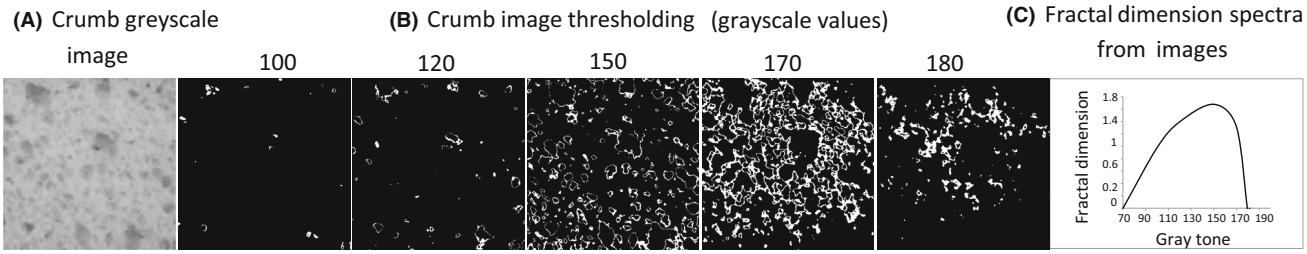


**Figure 2** An example of image processing. (A) A greyscale image of a control crumb. (B) Segmented images that show structure patterns of crumbs thresholded at different grey values. (C) The plot shows the obtained spectrum of a fractal dimension from each image.

statistical learning theory, which is commonly used for spectral data analyses (Boser *et al.*, 1992). *PCA* was used to study the differences between crumb structures from whole slices (Fig. 4a) and their zones, while *SVM-R* was applied to study the relationship among the crumb structure, moisture and textural properties of the two single slice zones during storage by evaluating calibration coefficients ($R^2$) and the root mean square error (RMSE). Studies were carried out with the toolbox application in the Matlab 7.6 environment (The Mathworks, Natick, Massachusetts, USA) PLS-Toolbox, 6.3 (Eigenvector Research Inc., Wenatchee, Washington, USA).

## Results and discussion

### Fermentation phase

The impact of presence of the co-product on the fermentation phase was studied based on the analysis of the dough height evolution kinetics while this operation lasted. The collected data and fitted models are represented in Fig. 3, and the generated Gompertz parameters are provided in Table 1 (*Fermentation phase*). The curves included in this figure show the maximum height at 60 min for the pure wheat formula. Height lowered following the increment in the substitution level with the co-product. Non-significant differences in the 5% and 10% substitution levels were found. They reached around 77.4% of the maximum height ($H_{max}$) of the control, while it was significantly less for 20%, which was a 65.2% (Table 1). Not differences were observed for velocity ($V_H$) for the substituted formulas, while the control one presented the highest one. The latent time ($L_t$ $_H$) was maximum for 10% and 20%, followed by 5% and the control with no differences.

The observed reduction in the gas retention capacity of doughs took place due mainly to two causes: lack of gluten because of the substitution of dry matter from the wheat flour; the interferences produced in the optimum gluten network formation by the co-product

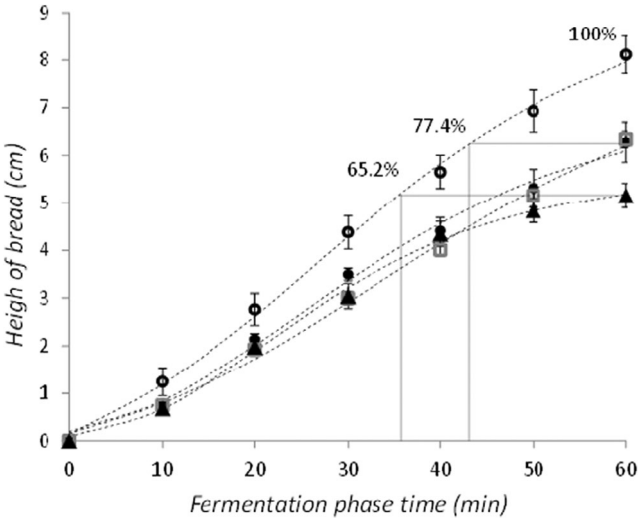


**Figure 3** The dough height evolution kinetics during the fermentation time. Dots mark the means of the observed data and bars denote standard deviation. Dotted lines mark the fitted model by the Gompertz equation. The series correspond to: ○ pure wheat; ● 5%, □ 10%, ▲ 20%. Values on the curve of the control indicate the percentage of its maximum height reached by the substituted formulas.

particles. Presence of insoluble fibre in dough-making limited air being incorporated into the dough matrix during mixing and then bubble nucleation, as well as $CO_2$ retention produced by yeast in the fermentation (Purić *et al.*, 2020). These observed differences have to be taken into account because of the implication of structural changes in dough matrixes, which could affect their thermal properties given the differences in the gas fraction, and then in the baking phase and the end bread properties.

### Baking phase

During this phase, the fermented dough underwent increased temperature, by which the retained gas expanded and mass varied mainly because of water

**Table 1** Results of the fermentation, baking and tempering and storage phases

| Substitution (% d.b) | Fermentation phase | | | Baking phase | Analytical determinations of breads | | | | Storage phase | | Correlation coefficients | | | |
|---|---|---|---|---|---|---|---|---|---|---|---|---|---|---|
| | $H_{max}$ (cm) | $V_H$ (cm/min) | $L_{t\ H}$ (min) | ΔM(%) | Sv ($cm^3$/g) | ΔSv (%) | Xw (g/g) | Xw/Sv (g/$cm^3$) | Day 3 Xw (g/g) | Day 6 Xw (g/g) | Xw $R^2$ | Xw RMSE | D $R^2$ | D RMSE |
| 0 | 7.9 ± 0.3c | 0.45 ± 0.01b | 4.5 ± 0.9a | 0.13 ± 0.01a | 3.38 ± 0.38c | – | 0.35 ± 0.01a | 0.10 ± 0.01a | 0.34 ± 0.002a | 0.3 ± 0.01a | 0.982 | 0.002 | 0.984 | 0.45 |
| 5 | 6.1 ± 0.4b | 0.37 ± 0a | 5.3 ± 0.1a | 0.13 ± 0.01a | 2.97 ± 0.16b | 12.3 | 0.36 ± 0.01a | 0.12 ± 0.01b | 0.35 ± 0.007ab | 0.32 ± 0.003b | 0.988 | 0.001 | 0.971 | 0.13 |
| 10 | 6.2 ± 0.1b | 0.34 ± 0.01a | 6.7 ± 0.6b | 0.12 ± 0.01a | 2.88 ± 0.18b | 14.9 | 0.361 ± 0.01a | 0.12 ± 0.01b | 0.36 ± 0.005bc | 0.35 ± 0.004c | 0.971 | 0.002 | 0.971 | 0.69 |
| 20 | 5.1 ± 0.2a | 0.37 ± 0a | 6.2 ± 0.5b | 0.13 ± 0.01a | 2.06 ± 0.4a | 39.0 | 0.36 ± 0.011a | 0.17 ± 0.02c | 0.366 ± 0.011c | 0.35 ± 0.003c | 0.989 | 0.007 | 0.986 | 0.65 |

Fermentation phase: $H_{max}$: maximum height (60 min), $V_H$: the maximum growth rate; $L_{t\ H}$: latency time before dough development begins. Baking phase: $\Delta M_{b\ max}$: maximum mass loss during baking time (35 min); $V_{\Delta M}$: is the maximum mass increment rate; $L_{t\ \Delta M}$: latency time before sample mass increment begins. Baking phase: $\Delta M$ mass increment at the end of bread cooling (30 min after the baking phase). Analytical determinations of breads: Sv: specific volume of breads; ΔSv: increment of specific volume compared to control breads; Xw: moisture of entire bread g water/grams of entire bread (crust and crumb); Xw/Sv: ratio of retained water per unit of specific volume. Correlation coefficients: *SVM-R* study between image information of crumb structure and moisture/hardness during storage of breads; $R^2$: calibration coefficient; *RMSE*: root mean square error of regression in g water/g crumb and *N* respectively. Different letters in the column indicate significant differences ($P < 0.05$). *d.b*, dry basis.

loss. These phenomena generate changes in the matrix that transforms fermented dough into bread by means of protein denaturalisation and starch gelatinisation, among others. These factors have a huge impact on the internal product structure, and then on its textural properties. The variation of mass ($\Delta M$) at the end of the cooling time after the baking phase was calculated (see the results in Table 1; *Baking phase*). In spite of the co-product having a significant impact on the fermentation kinetics in bread height ($H_{max}$) reduction terms, no differences in mass variation were observed. Breads ended this phase with the same mass loss, and then the same moisture ($Xw$) (Table 1). No formula showed any differences in mass variation ($\Delta M$), which was around 13% for them all. So although the co-product directly affected doughs' gas retention capacity in the fermentation phase, the mass variation in the baking phase was not affected by modifying dough morphology (height).

## Analytical determination of breads

*Specific volume*

Table 1 indicates the results (*Analytical determination of breads*). Differences in specific volumes were in accordance with the heights of doughs measured at the end of the fermentation phase. Any changes taking place during baking had no effect in this sense. The control samples reached the maximum $Sv$, followed by equal values for the 5% and 10% co-products. Finally, the 20% co-product presented maximum depletion and lost 39% of the control volume ($\Delta Sv$). This behaviour falls in line with other studies that have studied the effect of including insoluble fibre and bran in dietary fibre-enriched bread formulas, such as Curti *et al.* (2013) or Sciarini *et al.* (2017).

*Moisture*

Moisture ($Xw$) did not present differences, but followed the behaviour of the $\Delta M$. However, the co-product led to a significant increase in water retention per specific volume unit ($Xw/Sv$) (Table 1). The minor gas fraction in the substituted formulas should have favoured heat transport and then water loss. However, the water retention of the co-product appeared to compensate this fact. The results reported the overall conclusion that the co-product affected gas retention capacity, but not water retention, during processing, despite the implications that the morphological features of dough have during the heat treatment in the baking process.

*Crumb structure*

The generated multivariable data matrix based on fractal spectra was used to evaluate any differences among formulas by the *PCA*. The degree of

differentiation between formulas was studied by observing the scores generated from the two first principal components (*PCs*) and their distribution across the *PCA* space (Fig. 4a). Scores were distributed into four distinct groups across both *PC1* and *PC2*, which presented different coordinates depending on the

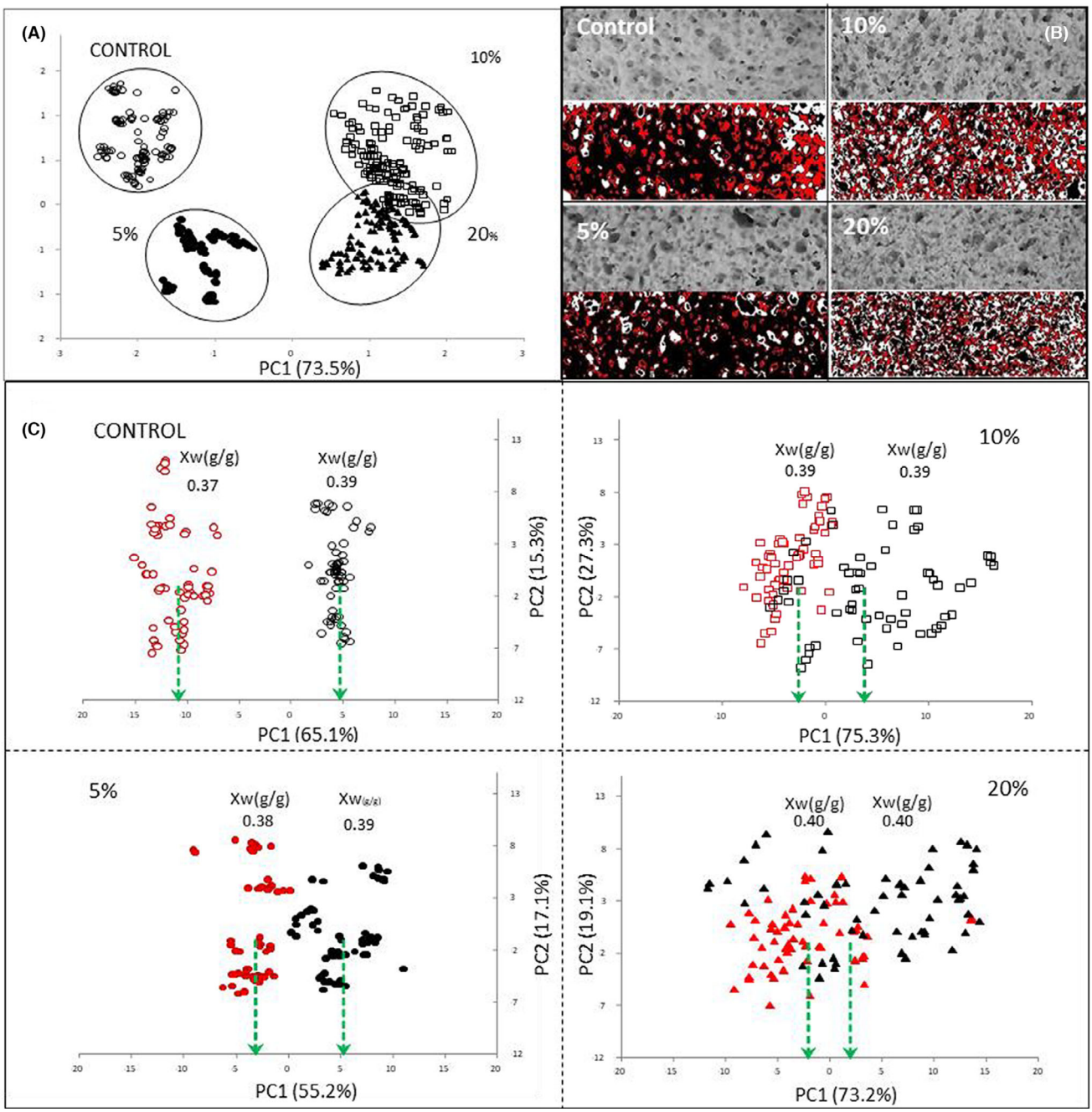


**Figure 4** The *PCA* space generated from the fractal spectra of crumbs. (A) PCA space of crumbs total. Circumferences include each formula. The series corresponds to: ○ pure wheat; ● 5%, □ 10%, ▲ 20%. (B) Examples of the segmented images of crumbs based on the grey values with maximum charges in the explained variance (loadings) of *PCA* in fig. a. White area, grey values of *PC1*; Red area, grey values of *PC2*. (C) The single *PCA* spaces generated from the fractal spectra of zones A (red series) and B (black series) of each formula. The series corresponds to the fig. A. Green dotted lines indicate the average *PC1* scores.

formula. The control had a separate position from the rest, as well as 5%. However, 10% and 20% appeared in a different position for *PC2*, but at the same one across *PC1*.

Positioning the formulas evidenced differences between crumb structures, although they tended to reduce the distance with increment or co-product proportion. To find the crumb zones responsible for these differentiations, the charges of each original variable (grey value) on the PC-loadings were calculated and the main peaks were selected. The selected grey values (*PC1* = 120–130 grey tone; *PC2* = 150 grey tone) were then used to segment the original images and to thus observe the influence zones for both *PC1* (white area) and *PC2* (red area) (Fig. 4b).

The formulas in Fig. 4b were positioned following the *PCA* space (Fig. 4a). The differences in the distribution of the coloured areas can be directly observed. It was hard to visually note the difference between the control and 5%, but from 10% the change in structures was highly marked. Moreover, 10 and 20% presented a strong increment in homogeneity in the structure distribution compared to the rest for both coloured areas. The co-product appeared to affect bubble formation because of the disruption of bubble-walls and bubble size. These observations match and explain the reduced gas retention previously observed in the fermentation phase.

The observed disruptions were not only physical causes, like those previously reported physicochemical effects of added fibres on gluten-starch-water relationships. The main disruption was the competition of fibre for water, which caused alterations to the correct dilution and hydration of the wheat components in the mixing phase, and thus resulted in anomalous structures (Alba *et al*., 2019).

This phenomenon was observed better throughout the micrographies of the crumb matrix structures. Some examples are included in Fig. 1b. We can see how co-product particles had incorporated into matrix structures, which affected the continuity of bubble walls. Martínez *et al*. (2014) have also published images about the impact of insoluble fibres on bread dough structures, which appeared almost unaltered in the dough matrix to become more rounded given the presence of starch granules, which led to irregular structures.

In this experiment, this factor affected the volume and crumb structures, but not mass loss. This fact implies that the water distribution in the crumb matrix should also be affected since the specific volume presented significant differences. To study the relationship between moisture and crumb structure, the distribution of moisture in bread crumbs was studied in two crumb zones, A and B.

The results are presented in Fig. 4c. Crumb zones (A and B) presented different moistures for the control formula and the 5% co-product. These differences were small following the % of co-product increment. The 20% co-product had the nearest and highest moisture values for both zones. The two zone models showed different slopes with % of co-product; the moisture of all the B zones was around 0.39–0.40, while A zones had different values, which ranged from 0.36 to 0.39 for the 0% and 20% co-product, respectively.

After observing these differences in crumb zone moistures, their relationship with crumb structures was studied by testing the differences between the structures of the A and B crumb zones separately. To this end, single *PCA* studies were done (four *PCA*s), but by taking the information of zones A and B as separate categories within each formula.

The generated *PCA* spaces are represented in Fig. 4c. This study reveals how zones were perfectly separated across PC1 for the control formula, and then the distance between them reduced following the increase in the co-product. To quantify this phenomenon, the difference between the average values of the PC1 scores (green dotted lines Fig. 4c) for zones A and B was calculated to compare moisture evolution.

The results showed how the moisture differences between zones A and B reduced following the increment in the co-product percentage, while the differences in PC1-scores A and B reduced at the same time. According to these results, the co-product effect conditioned both moisture distribution and the differences in the structures within crumbs. Thus a reduction in volume produced the homogenization of moisture across breadcrumbs and, in the same way, a reduction in the distances within PCA spaces, interpreted as a reduction in the structure differences among them.

Including the co-product led to changes in bread features, which caused differences in crumb moisture distribution and structures. Although structure and moisture distribution seemed related, it was necessary to reduce the scale of the crumb structure analysis for this to be evidenced. Following these results, the co-product impact on crumb structure conditioned the moisture distribution within each bread, but not the entire bread moisture because it was the same for them all. This conclusion is important to understand the behaviour of breads during storage.

### Storing breads

The results showed reduced mass loss of entire breads following an increased substitution level (Table 1). The co-product conferred breads high water retention, which was already observed on day 3. On day 6, the moisture of the breads with the 20% co-product was around 35%, while the control had 30% moisture.

This moisture retention did not different from most cereal brans and other fibre sources when they were included in bread doughs. To understand this effect on the crumb scale, the evolution of moisture and structure in crumb zones A and B was assessed following the same previous methods and by adding texture characterisation. Figure 5 shows the evolution of crumb hardness with the moisture of both crumb zones.

As a general effect, the increase in the co-product % generated greater hardness per unit of lost moisture, and showed four different models, for both zones A and B. A high substitution level produced greater hardness at a given moisture. Presence of the co-product led to harder crumbs with the same moisture content, mainly for 10% and 20%. The increment in breadcrumb hardness is stipulated as the response of starch component retrogradation (mainly amylopectin recrystallisation; Bosmans *et al.*, 2013) because of moisture loss. In this case, the results were contradictory because the formulas with the co-product presented higher moisture values, but also greater hardness. An explanation for increased hardness could be that the crumbs with the co-product had a lower gas fraction (lower specific volume), with greater firmness from day 0 due to lower porosity structures, and then density increased. Thus presence of the co-product produced firmer crumbs apart from moisture. These effects have already been observed in other studies into enriched fibre breads (Gallagher *et al.*, 2003; Sabanis *et al.*, 2009; Atzler *et al.*, 2021). Indeed, these results parallel the study of Curti *et al.* (2013), where bran-enriched breads present greater hardness, but also moisture. This suggests that in such bread formulas, moisture is not the main factor to influence hardness. The observed differences generated on crumb structures could play a key role to help understand these behaviours. Because of this, zones A (with a different moisture on day 0) (Fig. 5a) for the formulas with the co-product displayed the same evolution, while the control one showed a less marked hardness increment, but greater moisture reduction. Moreover, zones B (Fig. 5b) started with similar moisture, but presented progressively increasing hardness with % of co-product (slopes). This phenomenon matched the differences in crumb structures observed in Fig. 4c. It shows how bigger differences between crumb zone structures also had larger differences in the changed moisture-texture kinetics. When this relationship was explored by regression tests (*SVM-R*) between the moisture and hardness data *vs.* the structure data (imaging information) collected during storage, higher coefficients were obtained (Table 1: Correlation coefficients). This fact allowed us to assume that the close moisture-hardness relationship was also dependent on crumb structure evolution during storage. Thus by way of conclusion, although the co-product did not modify the moisture content in breads, it provided greater moisture retention during storage and changes in the crumb structure system, which led to a faster increase in hardness during storage.

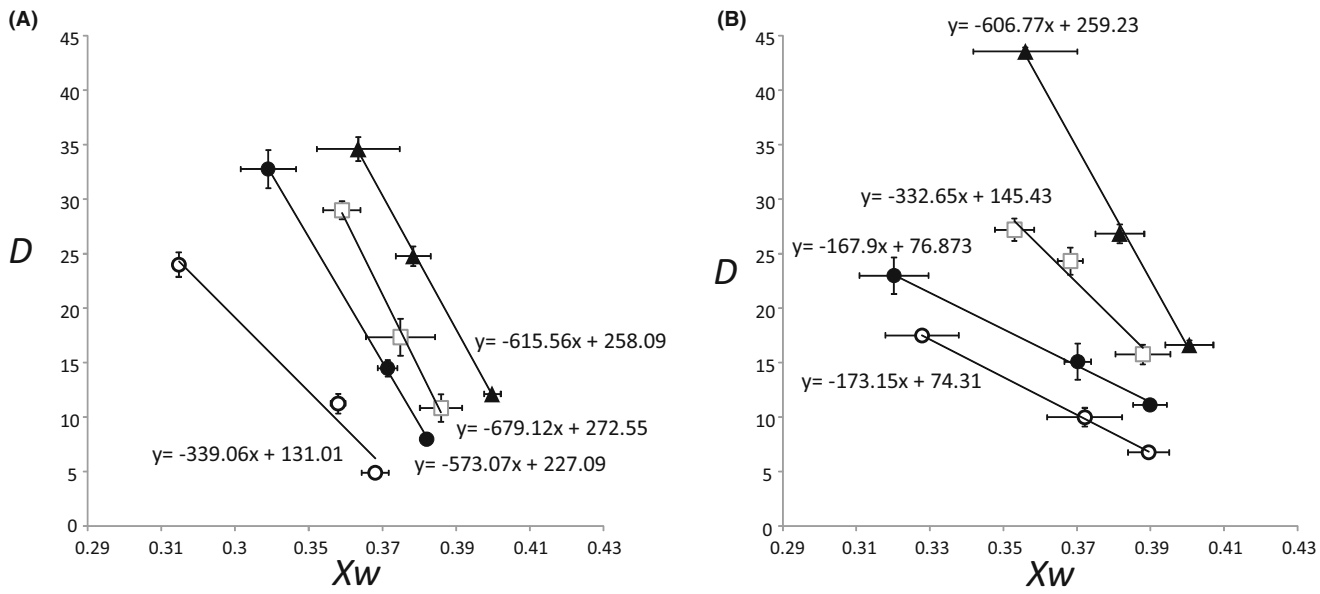


**Figure 5** Relationship of moisture (*Xw*) and hardness (*D*) in *N* of A crumb zones B and during storage. The series corresponds to: ○ pure wheat; ● 5%; □ 10%; ▲ 20%. Values on the lines indicate substitution levels. A letter means crumb zones. Bars indicate standard deviations.

## Conclusions

The tiger-nut milk co-product caused major modifications to dough behaviour and bread properties. It inclusion reduced dough development in the fermentation phase due to the disruption of an optimum starch-gluten net. The consequence of this effect was a significant reduction in the specific bread volumes; however, moisture at the end of the bread-making process was not affected. The internal bread structure was significantly modified. The co-product produced more homogeneous crumbs, along with a greater homogeneous moisture distribution. During storage, the co-product provided a higher moisture retention capacity. On the other hand, the changes generated in the structure properties increased faster the hardness of the crumb. The impact of the co-product on the crumb moisture-structure-texture system during storage was evidenced, where differences in structures seemed to condition moisture loss during storage and texture in the breadcrumb zones. The use of the tiger-nut milk co-product had a significant impact on both processing and the physicochemical properties of bread during storage, which has to be taken into account to enrich breads with fibre. More research is underway to control the observed effects, to obtain both favourable processing and bread properties, to make comparisons with other fibre sources and to evaluate the impact on sensory properties.

## Conflicts of interest

The authors declare no conflict of interest.

## Funding information

This study was supported by the Regional Valencian Ministry of Culture, Education and Sport for Scientific and Technological Politics by Project entitled "Use of non-wheat flours, from co-products of the food industry, to produce bread, cakes and snacks (AICO/2015/107)" and by the University Polytechnic of Valencia by program "Ayudas para la Contratación de Doctores para el Acceso al Sistema Español de Ciencia, Tecnología e Innovación, en Estructuras de Investigación de la UPV (PAID-10-17)".

## Author contributions

**Samuel Verdú:** Conceptualization (equal); formal analysis (equal); investigation (equal); methodology (equal). **Cecibel Alava:** Conceptualization (equal); data curation (equal); formal analysis (equal); investigation (equal); methodology (equal). **José M. Barat:** Conceptualization (equal); data curation (equal); funding acquisition (equal); project administration (equal). **conrado Carrascosa:** Conceptualization (equal); data curation (equal); formal analysis (equal); methodology (equal). **Raul Grau:** Conceptualization (equal); data curation (equal); funding acquisition (equal); investigation (equal); methodology (equal); project administration (equal).

## Peer review

The peer review history for this article is available at https://publons.com/publon/10.1111/ijfs.16248.

## Data availability statement

The datasets generated during the current study are not publicly available but are available from the corresponding author on reasonable request.

## References

Aguilar, N., Albanell, E., Miñarro, B., Guamis, B. & Capellas, M. (2014). Effect of tiger nut-derived products in gluten-free batter and bread. *Food Science and Technology International*, **21**, 1–9.

Alava, C., Verdú, S., Barat, J.M. & Grau, R. (2019). Enrichment of chips with fibre from a tiger-nut (Cyperus esculentus) milk co-product at 'source of fibre foods' and 'high fibre content foods' levels: impact on processing, physico-chemical and sensory properties. *International Journal of Food Science and Technology*, **54**, 908–915.

Alba, K., Campbell, G.M. & Kontogiorgos, V. (2019). Dietary fibre from berry-processing waste and its impact on bread structure: a review. *Journal of the Science of Food and Agriculture*, **99**, 4189–4199.

Alba, K., Rizou, T., Paraskevopoulou, A., Campbell, G.M. & Kontogiorgos, V. (2020). Effects of blackcurrant fibre on dough physical properties and bread quality characteristics. *Food Biophysics*, **15**, 313–322.

Atzler, J.J., Sahin, A.W., Gallagher, E., Zannini, E. & Arendt, E.K. (2021). Investigation of different dietary-fibre-ingredients for the design of a fibre enriched bread formulation low in FODMAPs based on wheat starch and vital gluten. *European Food Research and Technology*, **247**, 1939–1957.

Barros, J.C., Munekata, P.E.S., De Carvalho, F.A.L. *et al.* (2020). Use of tiger nut (Cyperus esculentus L.) oil emulsion as animal fat replacement in beef burgers. *Food*, **9**, 44.

Barros, J.H.T., Telis, V.R.N., Taboga, S. & Franco, C.M.L. (2018). Resistant starch: effect on rheology, quality, and staling rate of white wheat bread. *Journal of Food Science and Technology*, **55**, 4578–4588.

Bobreneva, I.V. & Baioumy, A.A. (2018). Effect of using tiger nuts (*Cyperus esculentus*) on nutritional and organoleptic characteristics of beef burger. *Bioscience Research*, **15**, 1424–1432.

Boser, B.E., Guyon, I.M. & Vapnik, V.N. (1992). A training algorithm for optimal margin classifiers. In: *Proceedings of the Fifth Annual Workshop on Computational Learning Theory*, Pittsburgh, July 1992, Pp. 144–152.

Bosmans, G.M., Lagrain, B., Fierens, E. & Delcour, J.a. (2013). The impact of baking time and bread storage temperature on bread crumb properties. *Food Chemistry*, **141**, 3301–3308.

Chu, K.H. (2020). Fitting the Gompertz equation to asymmetric breakthrough curves. *Journal of Environmental Chemical Engineering*, **8**, 103713.

Curti, E., Carini, E., Bonacini, G., Tribuzio, G. & Vittadini, E. (2013). Effect of the addition of bran fractions on bread properties. *Journal of Cereal Science*, **57**, 325–332.

De Melo, R.H.C. & Conci, A. (2013). How Succolarity could be used as another fractal measure in image analysis. *Telecommunication Systems*, **52**, 1643–1655.
Dhingra, D., Michael, M., Rajput, H. & Patil, R.T. (2012). Dietary fibre in foods: a review. *Journal of Food Science and Technology*, **49**, 255–266.
Gallagher, E., Gormley, T. & Arendt, E. (2003). Crust and crumb characteristics of gluten free breads. *Journal of Food Engineering*, **56**, 153–161.
Karperien, A. (2013). *FracLac for ImageJ [WWW document]. User's Guid. FracLac, V. 2.5*. Bathurst: Charles Sturt University. https://doi.org/10.13140/2.1.4775.8402
López-Azpiazu, I., Sánchez-Villegas, A., Johansson, L. *et al.* (2003). Disparities in food habits in Europe: systematic review of educational and occupational differences in the intake of fat. *Journal of Human Nutrition and Dietetics*, **16**, 349–364.
Martínez, M.M., Díaz, Á. & Gómez, M. (2014). Effect of different microstructural features of soluble and insoluble fibres on gluten-free dough rheology and bread-making. *Journal of Food Engineering*, **142**, 49–56.
Muñoz, S.E., del Pilar Díaz, M., Reartes, G.A. *et al.* (2022). The "diet model" and metabolic syndrome components: results from the Cordoba health and dietary habits investigation. *Nutrition*, **102**, 111739.
Panigrahy, C., Seal, A. & Mahato, N.K. (2020). Image texture surface analysis using an improved differential box counting based fractal dimension. *Powder Technology*, **364**, 276–299.
Purić, M., Rabrenović, B., Rac, V., Pezo, L., Tomašević, I. & Demin, M. (2020). Application of defatted apple seed cakes as a by-product for the enrichment of wheat bread. *LWT*, **130**, 109391.
Sabanis, D., Lebesi, D. & Tzia, C. (2009). Effect of dietary fibre enrichment on selected properties of gluten-free bread. *LWT - Food Science and Technology*, **42**, 1380–1389.
Sánchez-Zapata, E., Fuentes-Zaragoza, E., Fernández-López, J. *et al.* (2009). Preparation of dietary fiber powder from tiger nut (Cyperus esculentus) milk ("horchata") byproducts and its physicochemical properties. *Journal of Agricultural and Food Chemistry*, **57**, 7719–7725.
Sciarini, L.S., Bustos, M.C., Vignola, M.B., Paesani, C., Salinas, C.N. & Pérez, G.T. (2017). A study on fibre addition to gluten free bread: its effects on bread quality and in vitro digestibility. *Journal of Food Science and Technology*, **54**, 244–252.
Sun, J., Fu, J., Wang, Y., Ye, H., Wu, D. & Shu, X. (2019). Endogenous rice endosperm hemicellulose slows in vitro starch digestibility. *International Journal of Food Science and Technology*, **54**, 734–743.
Verdú, S., Vásquez, F., Ivorra, E., Sánchez, A.J., Barat, J.M. & Grau, R. (2015). Physicochemical effects of chia (salvia Hispanica) seed flour on each wheat bread-making process phase and product storage. *Journal of Cereal Science*, **65**, 67–73.
Verdú, S., Vásquez, F., Ivorra, E., Sánchez, A.J., Barat, J.M. & Grau, R. (2017). Hyperspectral image control of the heat-treatment process of oat flour to model composite bread properties. *Journal of Food Engineering*, **192**, 45–52.
Zheng, H., Jiang, L., Lou, H., Hu, Y., Kong, X. & Lu, H. (2011). Application of artificial neural network (ANN) and partial least-squares regression (PLSR) to predict the changes of anthocyanins, ascorbic acid, Total phenols, flavonoids, and antioxidant activity during storage of red bayberry juice based on fractal ana. *Journal of Agricultural and Food Chemistry*, **59**, 592–600.

## Supporting Information

Additional Supporting Information may be found in the online version of this article:

**Appendix S1.** Supporting Information.